Deep Mining 2024 – P Andrieux & D Cumming-Potvin (eds)

doi:10.36487/ACG_repo/2465_50

Model calibration and seismic potential vulnerability assessment with the mining rock mass seismicity model

Ronald Lachenicht [a,*], **Glenn Sharrock** [a]

[a] *ITASCA, Australia*

Abstract

The mining rock mass seismicity (MRS) model establishes modelled versus observed seismic potential correlation relations used to forecast the future rock mass seismic response to mining. ITASCA's FLAC3D continuum code calculates the plastic work dissipated throughout the rock mass and along geological structures for each mining extraction increment of a global mine model. The progressive failure and disintegration of the rock mass is modelled with different FLAC3D constitutive models. The understanding of the rock mass and geological structural environment in conjunction with available calibration data forms the foundation of the seismic potential assessment. Confidence associated with the derived calibration relations reflects the understanding and definition of the failure mechanics incorporated into the modelling.

This paper extends the MRS model calibration and seismic potential assessment methodology through the incorporation of modelled system response tests to assess the global system's vulnerability to failure. Strength assumptions are lowered during a model system test, reducing the analysis reliance on the accuracy of the input parameter assumptions. Spatial and temporal comparisons between the base modelled system response, modelled system tests and observed seismicity are used to refine the modelled seismic potential of failure regions. Failure responses identified from modelled calibration system tests can be integrated back into the baseline model, improving the derived calibration relations and model confidence. System tests are further applied to forward analyses to examine the ongoing system vulnerability to failure. The introduction of system tests with bracketing parameter ranges reduces the model reliance on deterministic input parameter assumptions, facilitating the incorporation of additional mitigation strategies for identified system test vulnerabilities associated with a high modelled seismic potential.

Keywords: *seismicity, model calibration, seismic potential assessment*

1 Introduction

Brady & Brown (2005) discuss the considerations of mine global stability where the requirement is to make sure that any small change in the equilibrium state of loading in a structure cannot provoke a sudden release of energy or a large change in the geometry of the structure. Analysis of modelled energy has historically been the foundation of the analysis of seismic instability in the mining industry, commencing with the concept of energy release associated with the incremental enlargement of tabular excavations (Cook et al. 1966). Jager & Ryder (1999) found the number of rockbursts per area mined to be proportional to the energy release rate (ERR) where ERR was calculated from the ratio of strain energy release to area mined. This concept was later extended to 3D pillar geometries by Wiles (2005) through the determination of local energy release density (LERD) being the area under the load deformation curve divided by the pillar volume. The MRS model builds on the concepts of ERR and LERD with the calculation of modelled plastic energy release over variable volumes directly correlated to the observed seismic response within each volume.

* Corresponding author. Email address: rlachenicht@itasca.com.au

2 Mining rock mass seismicity model

The MRS model can be broken down into the following main components:

- failure mechanisms
- constitutive models
- modelled seismic energy release potential calculation
- model damage calibration
- modelled seismic potential calibration
- forecasting modelled seismic potential.

2.1 Failure mechanisms

A seismic event is a sudden inelastic deformation within a given volume of rock, i.e. a seismic source, that radiates detectable seismic waves (Mendecki et al. 1999). As such, a critical foundation of modelling the seismic response of the rock mass is to encapsulate appropriate failure mechanisms into the numerical model. Figure 1 illustrates seismicity and damage mechanisms incorporating the potential for strainbursts, buckling, face crush bursts, pillar bursts and fault rupture energy release after Ortlepp (1997). Figure 2 illustrates the influence of stress and structure on rock mass failure modes after Diederichs (1999). In continuum models like FLAC3D (ITASCA 2024), failure mechanisms need to be encapsulated through robust estimations of rock quality parameters together with the explicit incorporation of relevant large to medium scale structures using zone joints. Discontinuum models like 3DEC or PFC3D (ITASCA 2024) can explicitly encapsulate a detailed jointing understanding of the rock mass as illustrated in Figure 2.

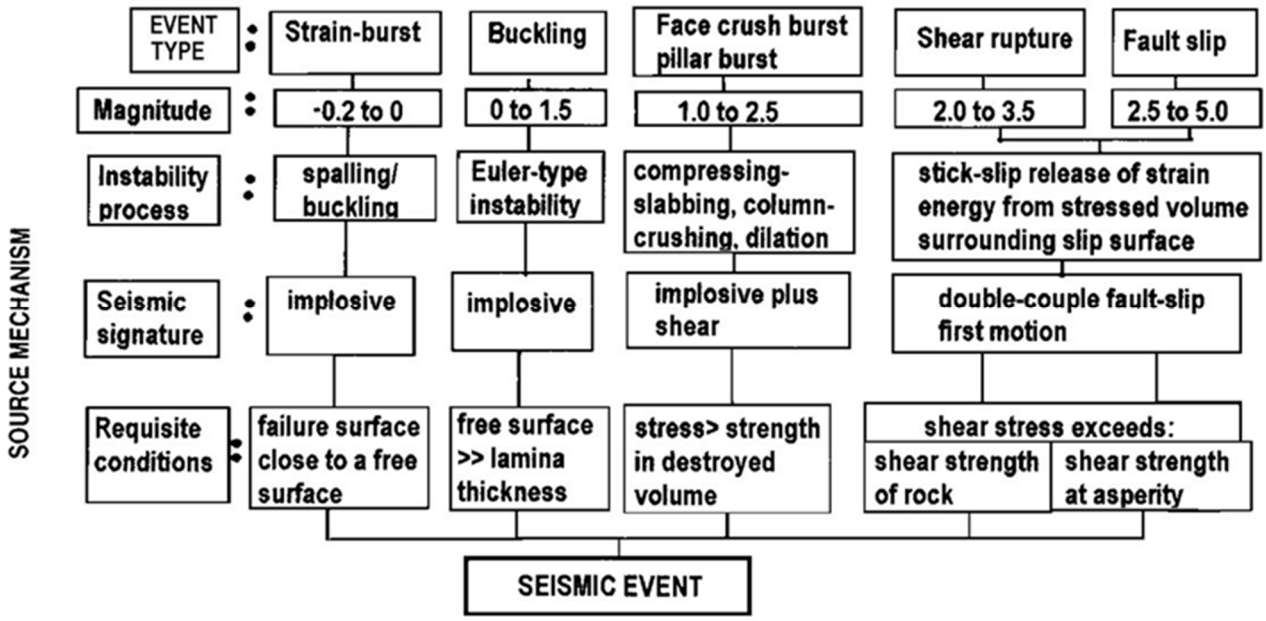

Figure 1 Seismicity and damage mechanisms in underground mines (Ortlepp 1997)

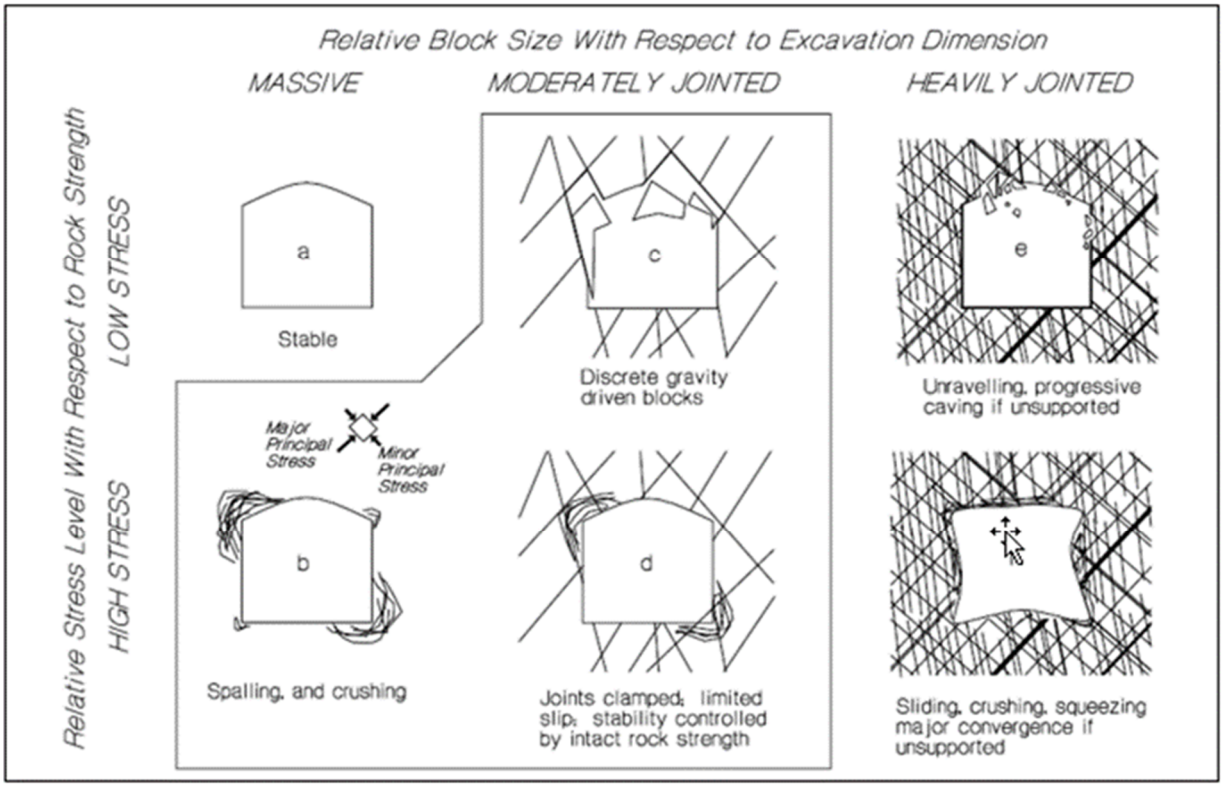

Figure 2 Influence of stress and structure on rock mass failure modes after Diederichs (1999)

2.2 Constitutive models

Within the FLAC3D continuum model the constitutive relations provide a mathematical description of the rock mass behaviour. The ITASCA model for advanced strain softening (IMASS) and strain softening/hardening ubiquitous-joint (SUBI) constitutive models have been applied for the MRS model.

2.2.1 ITASCA model for advanced strain softening (IMASS)

As part of the International Caving Study (Lorig 2000) and Mass Mining Technology (Chitombo & Pierce 2012) projects, several guidelines have been developed to capture the key mechanisms associated with caving in a numerical model and are summarised by Pierce (2013). IMASS has been developed by ITASCA based on these guidelines and aims to simulate the progressive failure and disintegration of the rock mass from an intact/jointed material to a caved material.

The peak strength envelope is described by the Hoek–Brown failure criteria (Hoek et al. 2002). The residual strength is typically that of a bulked rockfill (zero cohesion and a friction angle of 43 degrees). As the material yields, the strength is degraded by linear interpolation between the linear Mohr–Coulomb fit at peak and residual states based on the current stress state.

IMASS has been developed to represent the rock mass response to stress changes (i.e. rock mass yield, modulus softening, density adjustment, dilation, dilation shut-off, scaling of properties to zone size, cohesion weakening, tension weakening and frictional strengthening). This constitutive model was developed using strain softening material models, with strain-dependent properties adjusted to reflect the impacts of dilation and bulking as a result of induced stress changes. In IMASS, the geological strength index, m_i, and uniaxial compressive strength parameters control the shape of the peak Hoek–Brown envelope, which is defined in Hoek et al. (2002).

2.2.2 Strain softening/hardening ubiquitous-joint (with pre-peak strain hardening)

The bilinear SUBI model is a generalisation of the ubiquitous-joint model. In the bilinear model, the failure envelopes for the matrix and joints are the composite of two Mohr–Coulomb model criteria with a tension cutoff that can harden or soften according to specified laws. A non-associated flow rule is used for shear plastic flow and an associated flow rule is used for tensile-plastic flow (ITASCA 2024).

Within the SUBI constitutive model, zone-based matrix and joint properties are specified. Each of these property sets (matrix and ubiquitous joints) can fail in tension and shear independently of one another.

The strain softening model is based on the Mohr–Coulomb constitutive model; however, the cohesion, friction angle, tensile strength, modulus and dilation angle for the rock mass may be changed depending on the amount of plastic shear strain that has occurred in each model zone. The peak strength envelope is described by the Hoek–Brown failure criteria (Hoek et al. 2002) as approximated by a bilinear Mohr–Coulomb fit.

For the MRS model, the SUBI model has been modified to incorporate a strain hardening response of the rock mass. In Figure 3, strain hardening occurs between points A-B in the pre-peak portion of the rock mass stress-strain relation. After the peak strength of the rock mass is exceeded, strain softening occurs. Incorporation of the SUBI strain hardening constitutive model allows for improved modelling of the seismic response of a strong and brittle rock mass, where fracture initiation of the rock and associated seismic release can occur during the strain hardening phase prior to the rock mass reaching the peak strength envelope. This concept is illustrated in Figure 4 from Diederichs (2003).

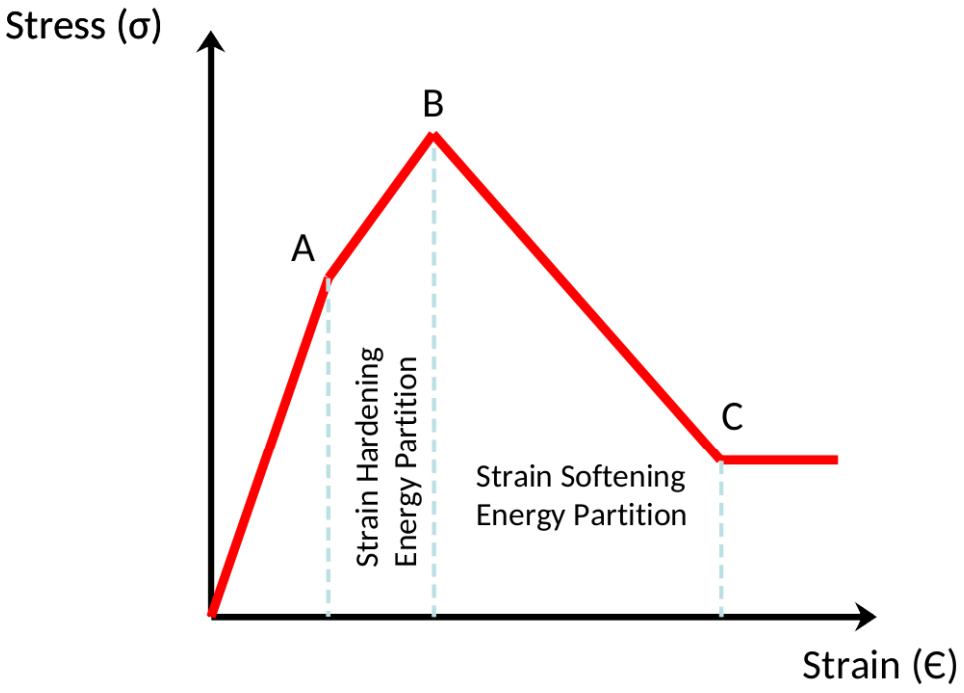

(A) Yield point initiation of seismicity (plastic strain = 0)
(B) Peak Strength
(A-B) Yielding with strain hardening - permanent damage (crack coalescence)
(B-C) Yielding with strain softening
(C) Residual strength reached at critical plastic strain

Figure 3 Conceptual SUBI constitutive model incorporating a pre-peak strain hardening response of the rock mass

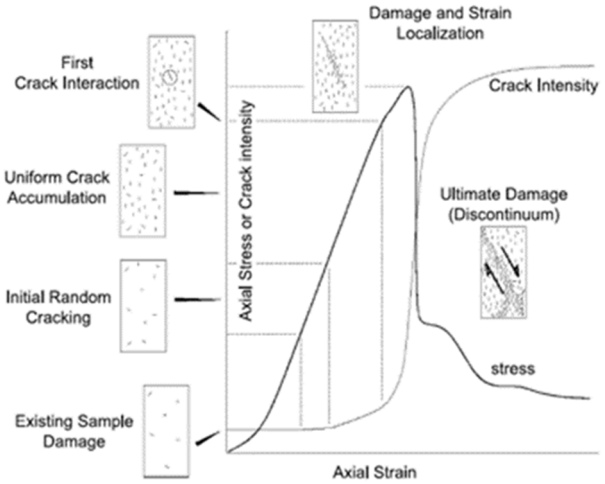

Figure 4 Stages of damage within a bonded disc model, representative of actual laboratory test samples from Diederichs (2003)

2.3 Modelled seismic energy release potential calculation

In FLAC3D (ITASCA 2024), elastic strain energy and dissipated plastic energy can be tracked for zones containing a mechanical model. FLAC3D uses an incremental solution procedure: the equations of motion (at the grid points) and the stress-strain calculations (at the zones) are solved every timestep. In the stress-strain equations, the incremental change in energy components is determined and accumulated as the system attempts to reach equilibrium.

As discussed in Section 2.2, several plasticity models are available in FLAC3D which can describe the deformability of the zones. Energy is dissipated through plastic work as the zones undergo irreversible deformation. The strain in any zone can be divided into elastic and plastic parts. The total shear plastic work dissipated during a timestep (dissipated plastic energy [DPE]) is the difference between the total shear energy and the elastic shear energy change at any timestep. The SUBI and IMASS constitutive models track plastic strain and energy release from the zones as a resultant of material failure, plastic shear deformation and slip occurring along ubiquitous joints. DPE density (DPED) is calculated from the total plastic shear work dissipated at each timestep by dividing the calculated plastic shear work dissipated in a zone by the volume of the zone.

The MRS model utilises DPE and DPED to assess the rock mass seismic potential. The concept of DPE is outlined in Figure 3. Energy is initially released while strain hardening occurs between points A-B (Figure 3) in the pre-peak portion of the rock mass stress-strain relation. After the peak strength of the rock mass is exceeded, strain softening occurs with further energy release. The modelled potential seismic energy release of the rock mass ends once a threshold of rock mass strain is exceeded prior to reaching the rock mass critical strain (at zero cohesion – point C in Figure 3). The seismic potential of explicitly modelled geological structures are integrated into the assessment through the calculation of plastic work done from modelled deformation along structures.

The basis of the DPE calculation is demonstrated in Figure 4 (after Diederichs 2003), showing the stages of damage within a laboratory test sample versus crack intensity. Initially calibration of DPE is undertaken using the onset of rock mass seismicity to identify the yield point A and the cessation of seismicity to identify the peak plastic seismic strain (Ɛps_seismic) between points B and C.

During the process of rock mass failure and fracture generation, energy is absorbed. Following from Brady & Brown (2005), if the DPED exceeds the rate at which energy can be non-violently absorbed then a rockburst hazard might exist. Higher intensity DPED and associated DPE occurring over large continuous volumes represent an increased seismic potential which infers the increased probability of an event equal to or exceeding a certain size occurring within the modelled time period.

2.4 Model damage calibration

Model damage calibration is undertaken against available surface deformation data, underground closure monitoring data and observations of damage in relation to damage mapping categories. Large-scale models incorporate the lithology, alteration and structural models, excavation layout and extraction sequence, together with an estimation of the in situ stress field and rock mass, and structure strength parameter assumptions. Model analyses are undertaken across a range of closure or damage categories at different points in time until an acceptable modelled versus observed match is attained. The key point in this step of the analysis is to demonstrate that the model exhibits a closure and damage response supported by available observational and monitoring data. Once this is achieved the model damage calibration is deemed acceptable and the model is ready to progress to the seismic potential calibration step of the MRS method. Adjustments to strength parameter assumptions and the introduction of additional failure mechanisms (e.g. foliation) may be required to attain an acceptable model damage calibration.

2.5 Modelled seismic potential calibration

Elastic numerical models can be utilised as an initial estimate of the seismic potential of a mine layout. These are associated with limited model assumptions and are fast to run. Seismic potential is assessed based on stress and strength criteria providing an initial assessment of the likelihood and severity of seismicity, e.g. rock mass damage and strainburst potential stress-strength categories defined by Castro et al. (2012).

Ortlepp (1997) defines a rockburst as a seismic event which causes violent and significant damage to tunnels and other excavations in the mine. Seismic events arise from conditions of unstable equilibrium, and involve the release of stored strain energy and the propagation of elastic waves through the rock mass (Brown 2007) where:

- The induced stresses must be high enough to induce slip on a pre-existing discontinuity (e.g. a fault) or fracture of the rock.
- The resulting slip or fracture must be mechanically unstable, releasing energy that cannot be absorbed in the processes of the slip or fracture themselves.

From the understanding developed, utilising elastic numerical modelling stress and strength criteria to assess a mine layout's seismic potential has limited value. The MRS model focuses on a non-linear approach, allowing the evolution of rock mass failure and released energy within a system to be captured and quantified.

The base MRS method uses the FLAC3D continuum software for the assessment of the seismic potential of complex mine layouts, but the formulation of the method is easily extended to incorporate discontinuum models embedded within a global FLAC3D model to emulate a more realistic structurally controlled failure response.

The seismic potential of a mine layout is assessed utilising non-linear methodologies calculated with FLAC3D. Modelled energy release with seismic potential is derived from modelled plastic energy release occurring under the following conditions:

- The yielding rock mass must be interlocked and not dilated to constitute seismic potential. A modelled plastic shear strain upper limit of 1.25% is assumed for the MRS method, as defined in Table 1.
- Seismic energy release of the rock mass must occur under conditions of high shear stress. The MRS methodology assumes a 20 MPa to 30 MPa maximum shear stress range (dependent on the local model calibration) to constitute a seismic potential.
- Geological structures need to be clamped and yielding under normal stress loading to represent a seismic potential in the MRS methodology. Normal stress criteria above 1 MPa are adopted, dependent on the local model calibration.

The MRS model assumes that modelled plastic energy release not meeting the above conditions manifests as non-seismic energy release. The total modelled seismic energy release potential within a volume is the sum of the calculated rock mass and explicit structure plastic energy release meeting the above criteria.

Table 1 Rock mass damage category relations to plastic shear strain and rock mass strength loss assumptions based on damage observations and bonded block modelling (Sharrock 2017)

Category	Plastic shear strain* (%)	Rock mass strength loss (%)	Rock mass response
A	0–0.50%	0–10%	Onset of fracturing/spalling/slabbing
B	0.50–1.25%	10–25%	Rock mass fractured but highly interlocked
C	1.25–2.50%	25–50%	Rock mass highly fractured, interlocked and dilated
D	2.50–5.00%	50–100%	Rock mass severely fractured and substantially dilated, with minimal interlocking
E	>5.00%	100%	Complete loss of strength - material in residual state

* Plastic shear strain and rock mass strength loss vary with geological strength index and zone size, and are indicative only

Seismic efficiency is defined as the ratio of the total energy radiated as seismic energy compared with the released energy (Brady & Brown 2005). The seismic efficiency relation is used to determine the proportion of modelled energy available for seismic release. McGarr et al. (1979) showed the seismic efficiency of the strain energy released during seismic events to be in the range of 1%. ITASCA back-analysis case studies of observed mine seismic data indicate a seismic efficiency range of 0.01% to 1% for a constant seismic efficiency assumption. Improved seismic potential calibration correlations have been attained using a variable seismic efficiency assumption where the seismic efficiency is increased relative to the level of the DPED present within individual modelled volumes: i.e. the higher the local energy concentration, the more energy will be available to be released seismically.

During model calibration the seismic efficiency assumption can be constrained through comparisons of time histories of the modelled seismic energy potential versus the observed seismic response. Figure 5 compares the modelled versus observed energy release over a large-scale calibration volume, showing that a seismic efficiency assumption of 0.15% is optimal for this case study.

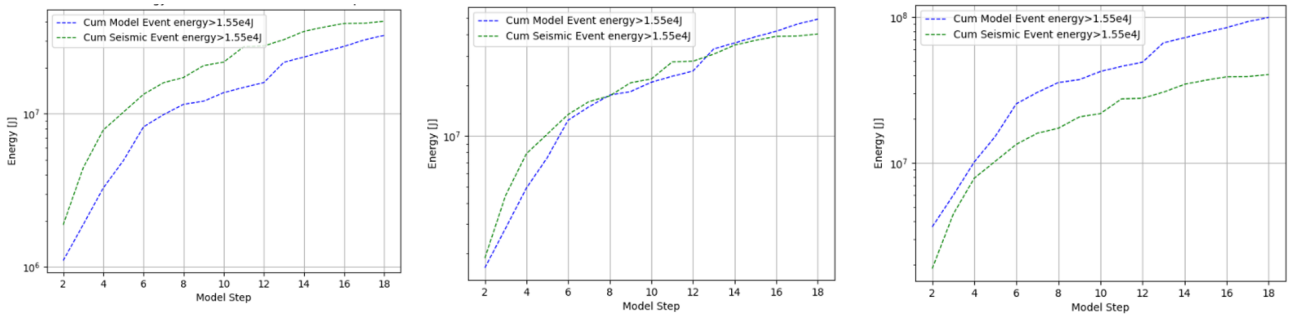

(a) (b) (c)

Figure 5 Comparison of the modelled versus observed energy release through time over a large-scale calibration volume for different seismic efficiency assumptions. (a) Seismic efficiency = 0.1%; (b) Seismic efficiency = 0.15%; (c) Seismic efficiency = 0.3%

Further quantification of the modelled seismic potential severity in the MRS method is attained from seismic source parameter relations using available seismic data at a site. Brownfield sites can directly interrogate available seismic source parameter relations while greenfield sites need to apply relations derived from sites with comparable conditions. Available seismic data is used to derive the following relations:

- Energy release versus moment magnitude relation (Figure 6).
- Source radius versus moment magnitude relation (Figure 7).

The energy release versus moment magnitude relation is used to define approximate seismic energy thresholds that need to be exceeded to support the viability of an equivalent moment magnitude event as defined by the least squares fit shown in Figure 6. Figure 6 shows an example case study analysis undertaken for a mine referred to as 'Mine A' in this paper. If an upper fit is applied a specified energy level will be associated with a relatively lower moment magnitude potential versus a lower fit associated with an equivalent higher moment magnitude potential dependent on the scatter surrounding the relation. Using this approach, modelled seismic energy release is correlated back to seismic moment magnitude, reducing the uncertainty associated with measuring seismic energy for an individual seismic event from a mine seismic system (Mendecki 2008).

The source radius versus moment magnitude relation is used to define approximate seismic source radius thresholds for equivalent moment magnitude event viability as defined by the least squares fit shown in Figure 7.

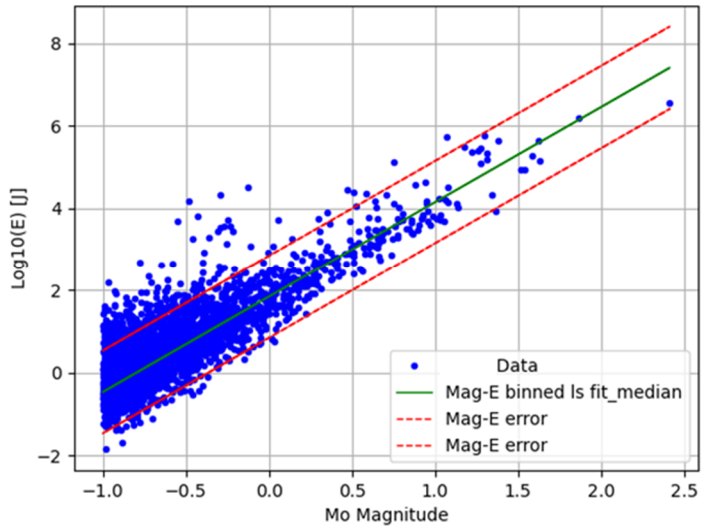

Figure 6 Log of seismic energy versus moment magnitude seismic relation for Mine A. The green line shows the least squares fit used for the MRS model calibration

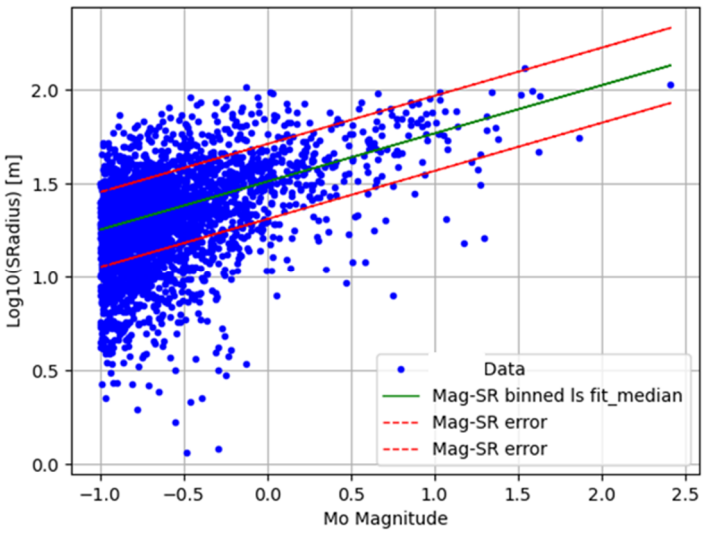

Figure 7 Log of seismic source radius versus moment magnitude seismic relation for Mine A. The green line shows the least squares fit used for the MRS model calibration

Table 2 shows a summary of seismic source volume, seismic energy release and moment magnitude thresholds derived from the median fits shown in Figure 7 and Figure 8. In the MRS model, the modelled energy release with an applied seismic efficiency assumption is cumulated over equivalent source volumes shown in Table 2 to assess if the energy thresholds are exceeded. The energy release versus moment magnitude relation sets the energy thresholds over equivalent source volumes for a modelled seismic potential release to be considered viable.

This assessment approach does not attempt to predict individual seismic events but provides an estimate of potential seismic release in a region based on the derived modelled energy output. The resultant estimate can be used by the design team to optimise mine layouts and extraction sequences, and to support design in regions with complementary closure, damage, seismic hazard and ground motion assessments. Note that the modelled seismic energy release potential could translate to a seismic response of many small events or a single large event. In addition, seismic release is sporadic in time and space, with events potentially occurring outside of the modelled analysis periods.

Table 2 Summary of seismic source volume, seismic energy release and moment magnitude thresholds derived for Mine A from available seismic source parameter relations over the calibration volume and applied to the mining rock mass seismicity model interpretation

Moment magnitude	Seismic energy (J)	Seismic source radius (m)
2.6	7.09e7	150
2.3	1.44e7	130
1.9	1.71e6	100
1.5	2.03e5	80
1.0	1.42e4	60
0.4	5.84e2	40

3 Mining rock mass seismicity model calibration

Once the seismic efficiency assumption and seismic moment thresholds are defined, the next step in the MRS model calibration process is to spatially compare modelled seismic potential versus observed seismic release. Figure 8 shows an example case study undertaken for a mine (referred to as ‘Mine B’ in this paper) of the spatial comparison between the radiated seismic energy of observed seismic events (spheres) and isovolumes of modelled seismic energy release potential incorporating a seismic efficiency assumption. Seismic efficiency assumptions can be fine-tuned during this calibration step within the limits of a large scale assessment as outlined in Figure 5.

Figure 9 shows an example model step for a case study analysis undertaken for a mine referred to as ‘Mine C’ in this paper comparing isovolumes of modelled seismic energy release potential to the moment magnitude of individual events occurring in that step.

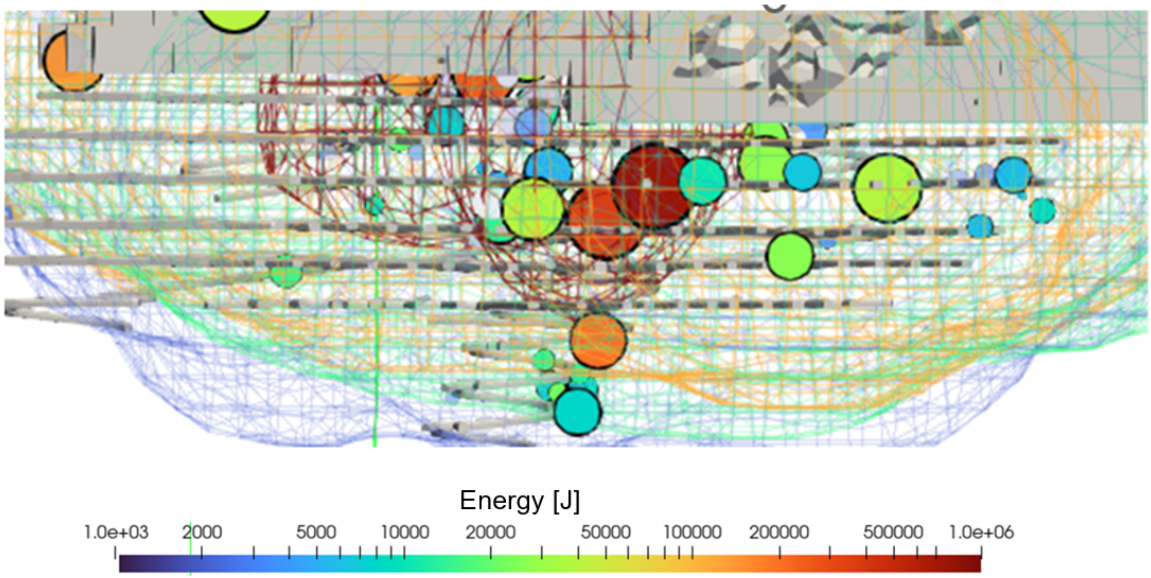

Figure 8 **Mine B spatial comparison between radiated seismic energy (spheres) and iso-volumes of modelled seismic energy release potential incorporating a seismic efficiency assumption**

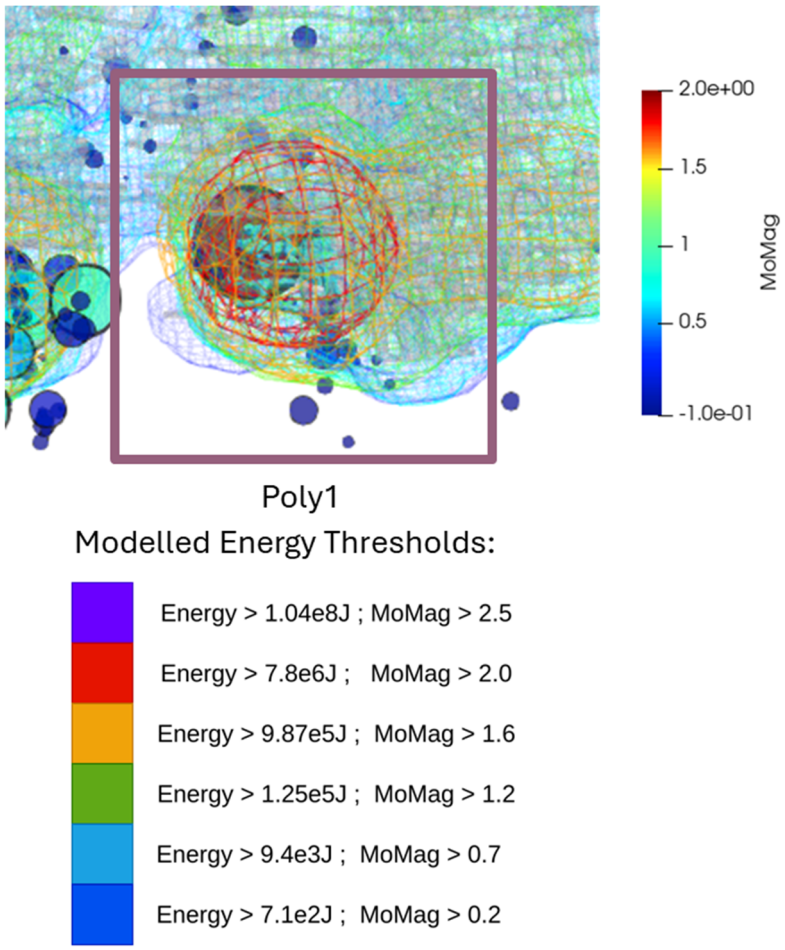

Figure 9 **Mine C spatial comparison between seismic moment magnitude (spheres) and isovolumes of modelled seismic energy release potential incorporating a seismic efficiency assumption. The isovolumes are colour-coded to derived energy-moment magnitude thresholds. Poly 1 depict spatial limits of filtering used for analysis in Figure 10**

Figure 10 shows time-history comparisons over the Poly 1 shown in Figure 9. The time-history analysis is used to rapidly assess concentrated energy release and the seismic potential within a selected volume. Cumulative time-history trends indicate how rapidly seismic energy potential is changing within the analysed volume prior to a seismic event occurrence.

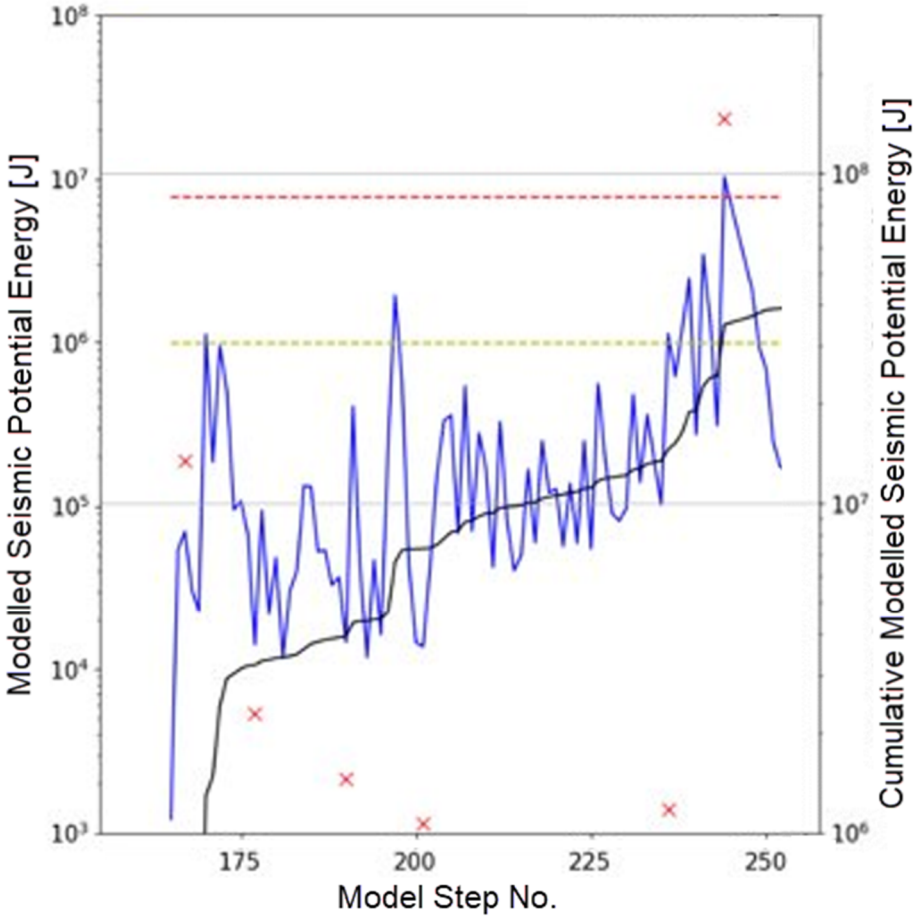

Figure 10 Mine C detailed time-history comparisons over Poly 1 (spatial extents shown in Figure 9). The horizontal red and yellow dashed lines indicate the energy thresholds equivalent to a moment magnitude 2.0 and 1.6 seismic potential. The blue line tracks the model seismic energy release potential and the black line the cumulative model seismic energy release potential within Poly 1, with the red crosses indicating individual seismic events energy releases during each period

Figures 11 and 12 show examples of statistically quantifying the MRS model calibration forecast accuracy extracted from mine calibration case studies referred to as 'Mine D' and 'Mine E' in this paper. The graphs show the probability that the model seismic energy release potential forecast captures the occurrence of observed individual seismic events above equivalent defined energy thresholds. The blue dots represent individual periods which show that in some cases all the seismic events occurring in that period were successfully captured, while in other cases less than 50% to none of the events were captured. The blue dashed lines average the probabilities across the time periods for each energy threshold analysed. Mine D indicates an overall forecast performance of 60% for energy thresholds less than 10^5 J, going up to 80% above 10^5 J. Mine E indicates an overall forecast performance in the vicinity of 50% across the energy ranges. As shown, the results vary from case study to case study and are dependent on factors such as failure mechanism understanding and rock mass strength variability. Calibration studies associated with low forecast probabilities can be re-assessed in terms of failure mechanism understanding with quantification of the impact on the resultant forecast probabilities.

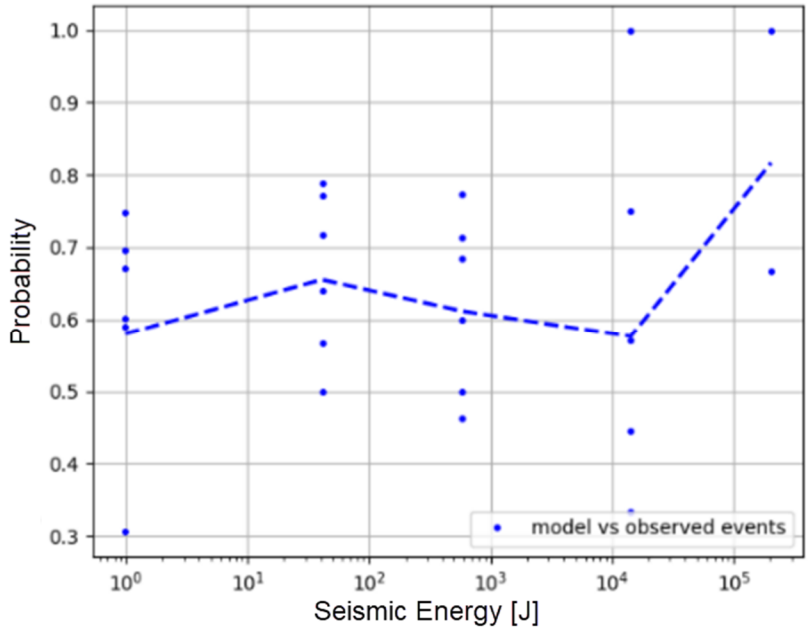

Figure 11 Probability that the model seismic energy release potential forecast captures the occurrence of observed individual seismic events above equivalent defined energy thresholds over monthly periods for Mine D

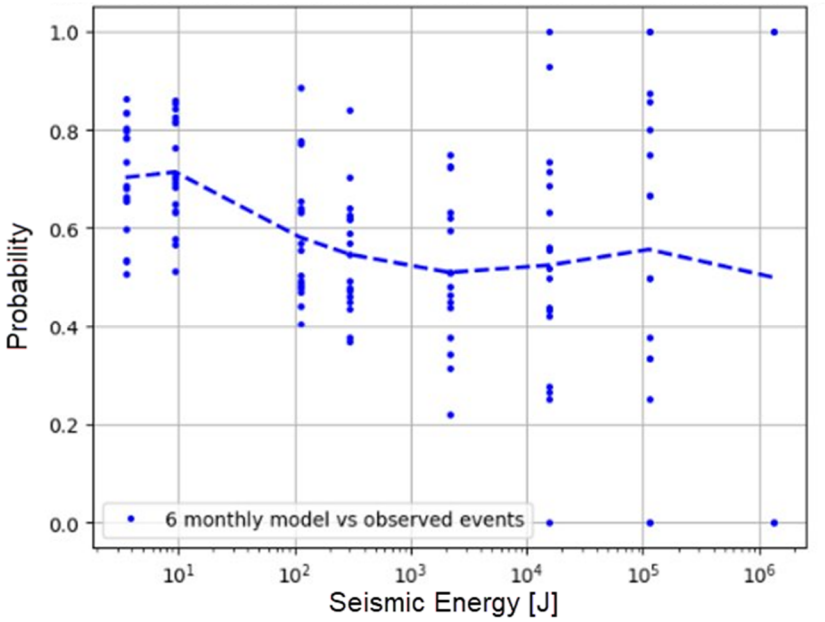

Figure 12 Probability that the model seismic energy release potential forecast captures the occurrence of observed individual seismic events above equivalent defined energy thresholds over monthly periods for Mine E

Figure 13 shows an example calibration case study (referred to as 'Mine F' in this paper) of a derived model seismic energy release potential versus observed seismic energy release relation. The green line represents a least square fit of median bin intervals, with the red and blue dashed lines the lower and upper quartile fit, respectively. Significant scatter is present across the model forecasts but an increasing trend with an overall matching scale is evident across the energy range.

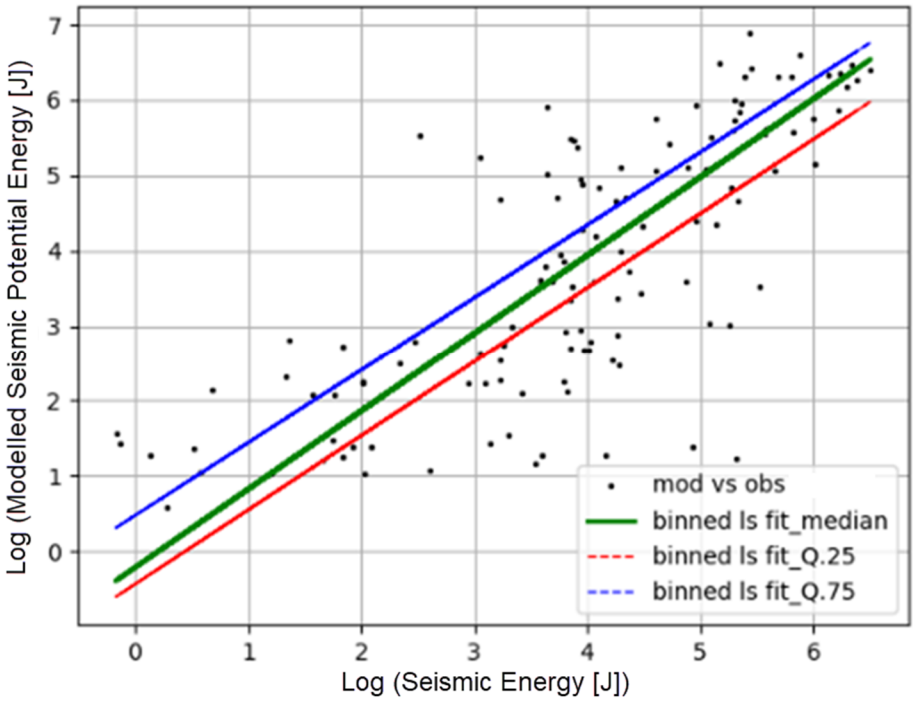

Figure 13 Mine F derived model seismic energy release potential versus observed seismic release relation

For the MRS calibration examples shown in Figures 11, 12 and 13, the model seismic energy release potential is derived from the application of the modelled seismic energy release potential criteria listed in Section 2 over selected volumes, without the application of any clustering algorithms to define a model seismic event occurrence. Seismic trigger potential is assessed based on energy continuity and concentration together with time-history trends. Modelled event clustering rules can be added as a more detailed analysis step to refine the initial results, build an understanding of the role played by the model failure mechanisms and improve design confidence (e.g. clustering based on strain tensor similarity).

4 Mining rock mass seismicity model extension

The accuracy of the model calibration approach outlined in Section 3 is dependent on the failure mechanisms and the input parameter assumptions incorporated in the model. Application of a model system test calibration approach can reduce the reliance on the accuracy of the input parameter assumptions. Slightly elevated strength assumptions can be initially selected, with a system test undertaken when the model versus observed response deviates. A system test involves a lowering of the strength assumption across the calibration area. Spatial and temporal comparisons between the base modelled system response, modelled system tests and observed seismicity can be used to refine the modelled seismic potential of failure regions. Failure responses identified from modelled calibration system tests can be integrated back into the baseline model, improving the derived calibration relations and model confidence. This modelling approach is analogous to the modelling and seismicity integration methods outlined in Wiles et al. (2001).

Figure 14 shows a calibration case study (referred to as ‘Mine G’ in this paper) example encompassing a variable strength rock mass where the model is yielding earlier than the observed response. Increasing the model strength assumptions results in an underestimation of the observed seismic response, presenting a difficult problem in defining an appropriate strength distribution present across the rock mass.

Implementation of a system test methodology within the MRS method improves the model calibration. Figure 15 shows the result of the Mine G model calibration where the modelled seismic energy potential time-history now closely matches the observed seismic energy release. Figure 16 quantifies the model seismic energy release potential versus observed seismic release relation over the calibration periods analysed for Mine G (Figure 15).

System tests are further applied to forward analyses to examine the ongoing system's vulnerability to failure. The introduction of system tests with bracketing parameter ranges reduces the model reliance on deterministic input parameter assumptions, facilitating the incorporation of mitigation strategies for identified system test vulnerabilities associated with a high modelled seismic potential.

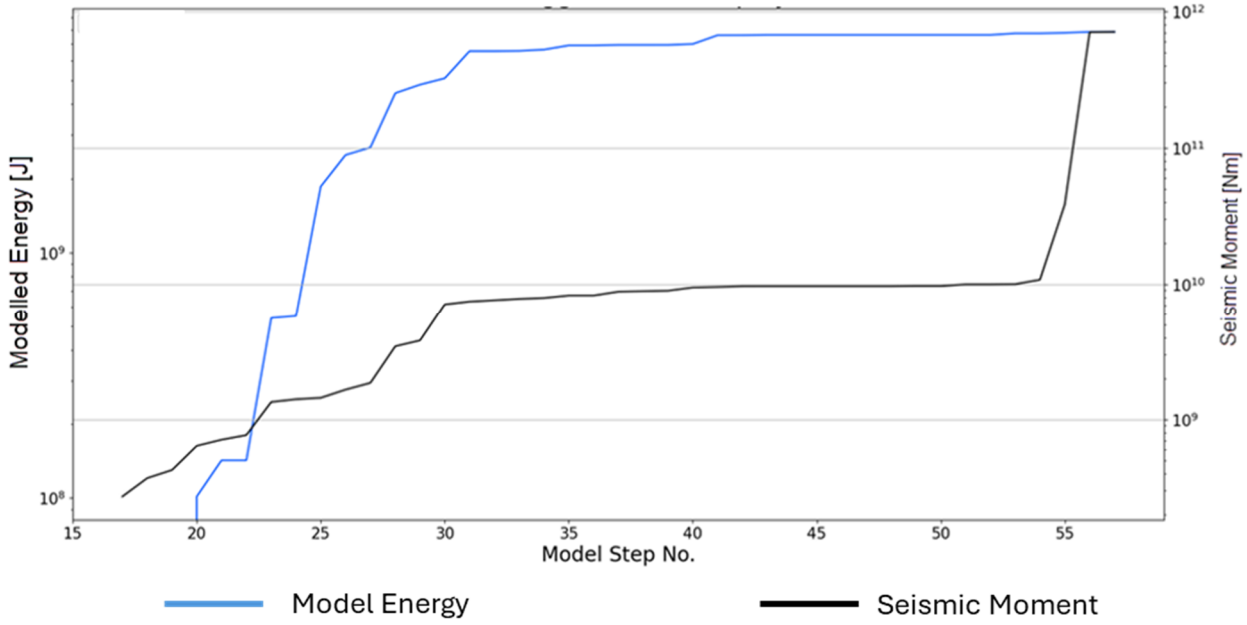

Figure 14 Mine G cumulative time-history comparison of modelled seismic energy release potential versus observed seismic moment. The model is yielding earlier than the observed seismic response

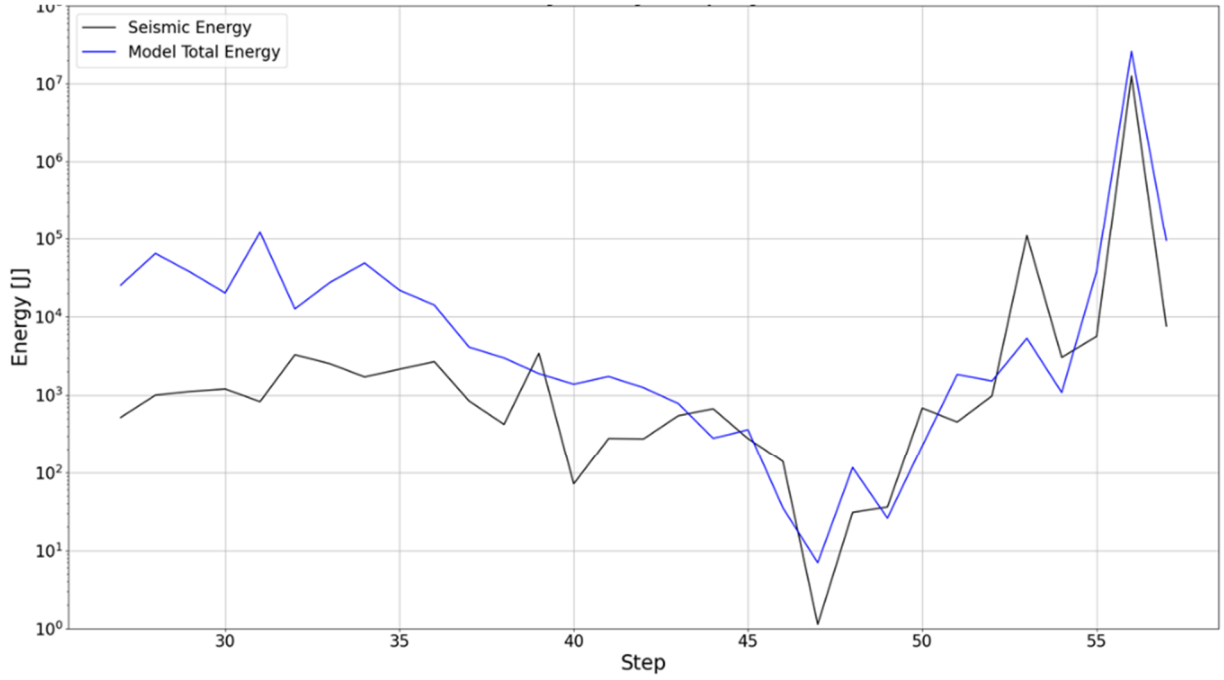

Figure 15 Mine G time-history comparison of the modelled seismic energy release potential versus the observed seismic energy release where the modelled seismic energy release potential time-history now closely matches the observed seismic energy release. The analysis incorporates a stronger rock mass assumption with system tests where large model versus observed deviations are evident during the model calibration.

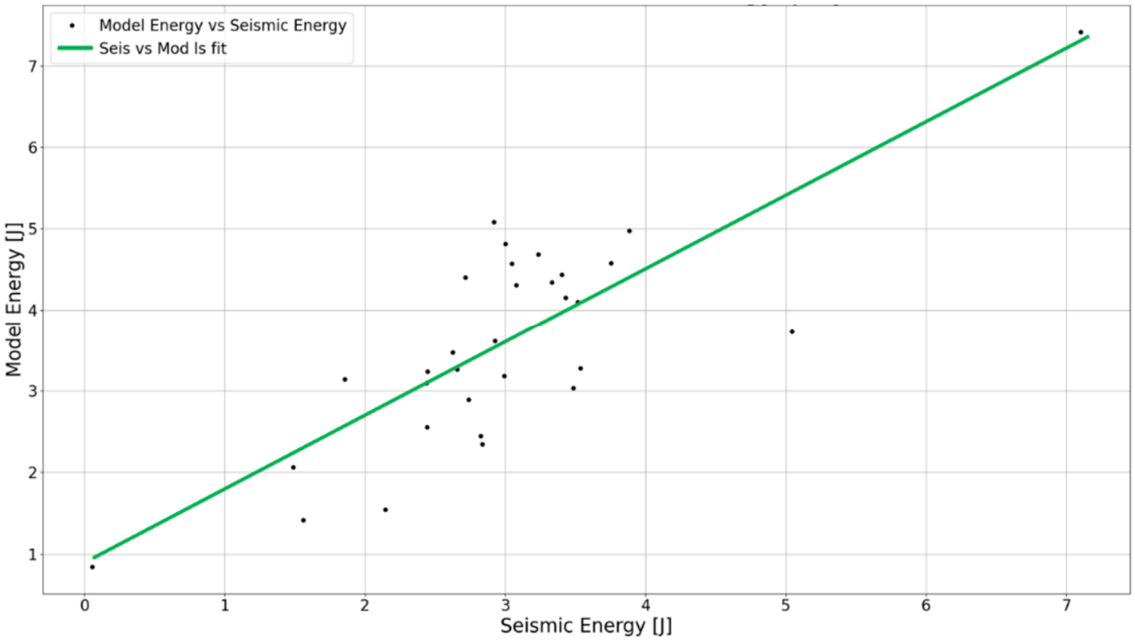

Figure 16 Mine G derived model seismic potential versus observed seismic release relation over the calibration periods shown in Figure 15

5 Conclusion

The MRS model's key design advantages are:

- a logical and consistent approach to assessing seismic potential of the rock mass
- clarity and transparency. The initial approach simplifies analysis complexity but allows for more detailed subsequent interrogation of the results
- applicability to problems which indicate a poor understanding of interpreted failure mechanisms. The results are measurable against the observed seismic response, allowing for refinement with a quantifiable assessment of the impact of changes to the inputs as understanding and information improves
- adaptability for a mine-wide scale analysis to gain a broad understanding of the seismic potential across a mine.

The MRS model assessment method utilises modelled seismic energy release potential as a basis for design guidance. The approach does not attempt to predict the occurrence of individual seismic events. It provides a broad estimate of seismic potential over a region, derived from modelled energy release. Temporal and spatial confidence in the resultant seismic energy release potential estimates can be quantified during model calibration. The resultant estimate can be used by a design team to optimise mine layouts and extraction sequences, and to design ground support complemented with assessments of closure, damage, seismic hazard and ground motion studies.

Application of a model system test calibration approach can reduce the reliance on the accuracy of the input parameter assumptions. The introduction of system tests with bracketing parameter ranges reduces the model reliance on deterministic input parameter assumptions, facilitating the incorporation of mitigation strategies for identified system test vulnerabilities associated with a high modelled seismic potential.

Acknowledgement

The authors would like to acknowledge Yoann Herbert for his contribution to many of the modelling algorithms used within the MRS method.

References

Brady, BHG & Brown, ET 2005, *Rock Mechanics for Underground Mining*, 3rd edn, Kluwer Academic Publishers, Dordrecht.

Brown, ET 2007, *Block Caving Geomechanics (The International Caving Study I, 1997-2000)*, *University of Queensland, JKMRC Monograph Series in Mining and Mineral Processing, Volume 3*, JKMRC, Indooroopilly.

Castro, LAM, Bewick, RP & Carter, TG 2012, 'An overview of numerical modelling applied to deep mining', *Innovative Numerical Modeling in Geomechanics*, CRC Press, Boca Raton.

Chitombo, G & Pierce, ME 2012, *A Practical Guide on the Use of the MMT Tools and Methodologies - Block Panel and Sublevel Caving*, report to Mass Mining Technology project.

Cook, NGW, Hoek, E, Pretorius, JPG, Ortlepp, WD & Salamon, MDG 1966, 'Rock mechanics applied to rockbursts', *Journal of the South African Institute for Mining and Metallurgy*, pp. 435–714.

Diederichs, MS 1999, *Instability of Hard Rockmasses: The Role of Tensile Damage and Relaxation*, PhD thesis, University of Waterloo, Waterloo.

Diederichs, MS 2003, 'Rock Fracture and collapse under low confinement conditions', *Rock Mechanics and Rock Engineering*, vol. 36, no. 5, pp. 339–381.

Hoek, E, Carranza-Torres, C & Corkum, B 2002, 'Hoek-Brown failure criterion - 2002 edition', *Proceedings of NARMS-TAC Conference*, University of Toronto Press, Toronto.

ITASCA 2024, *ITASCA Software Guide*, version 9.0.169, Minneapolis, https://docs.itascacg.com.

Jager, AJ & Ryder, JA 1999, *A Handbook on Rock Engineering Practice for Tabular Hardrock Mines*, Safety in Mines Research Advisory Committee, Johannesburg.

Lorig, L 2000, *The Role of Numerical Modelling in Assessing Caveabilty,* ITASCA, Minneapolis, report to the International Caving Study.

McGarr, A, Spottiswoode, SM, Gay, NC & Ortlepp, WD 1979, 'Observations relevant to seismic driving stress, stress drop and efficiency', *Journal of Geophysical Research*, vol. 84, pp. 2251–2261.

Mendecki, AJ 2008, 'Forecasting Seismic Hazard in Mines', in Y Potvin, J Carter, A Dyskin & R Jeffrey (eds), *SHIRMS 2008: Proceedings of the First Southern Hemisphere International Rock Mechanics Symposium*, Australian Centre for Geomechanics, Perth, pp. 55–69, https://doi.org/10.36487/ACG_repo/808_101

Mendecki, AJ, van Aswegen, G & Mountfort, P 1999, 'A guide to routine seismic monitoring in mines', in AJ Jager & JA Ryder (eds), A *Handbook on Rock Engineering Practice for Tabular Hard Rock Mines*, Creda Communications, Cape Town.

Ortlepp, WD 1997, *Rock Fracture and Rockbursts – An Illustrative Study*, South African Institute of Mining and Metallurgy, Johannesburg.

Pierce, M 2013, 'Numerical modeling of rock mass weakening, bulking and softening associated with cave mining', *ARMA eNewsletter*, Spring 2013, no. 9.

Sharrock, G 2017, 'Rock mass damage category relations based on damage observations and bonded block modelling', unpublished ITASCA memorandum.

Wiles, TD, Lachenicht, R & van Aswegen, G 2001, 'Integration of deterministic modelling with seismic monitoring for the assessment of rock mass response to mining: Part I Theory', *RaSiM5: Proceedings of the 5th International Symposium on Rockbursts and Seismicity in Mines*, South African Institute of Mining and Metallurgy, Johannesburg.

Wiles, TD 2005, 'Rockburst prediction using numerical modelling—realistic limits for failure prediction accuracy', in Y Potvin & M Hudyma (eds), *RaSiM6: Proceedings of the Sixth International Symposium on Rockburst and Seismicity in Mines Proceedings*, Australian Centre for Geomechanics, Perth, pp. 57–63, https://doi.org/10.36487/ACG_repo/574_0.5